Preparation of Siloxane–Silsesquioxane Hybrid Thin Films for Large-Scale-Integration Interlayer Dielectrics with Excellent Mechanical Properties and Low Dielectric Constants

Jin-Heong Yim,[1] Yi-Yeol Lyu,[1] Hyun-Dam Jeong,[1] Sang Kook Mah,[1] Jingyu Hyeon-Lee,[1] Jun-Hee Hahn,[2] Gwang Seok Kim,[3] Seok Chang,[1] Jae-Geun Park[1]

[1]*E-Polymer Laboratory, Samsung Advanced Institute of Technology, San 14-1, Nongseo-ri, Kiheung-eup, Yongin-shi, Kyungki-do, 449-712, Korea*
[2]*Korea Research Institute of Standards and Science, P.O. Box 102, Yusong, Taejon, 305-600, Korea*
[3]*Materials Processing Laboratory, Department of Materials Engineering, Hankuk Aviation University, Koyang, Kyungki-Do, 412-791, Korea*

Received 8 July 2002; accepted 6 January 2003

ABSTRACT: Several kinds of homogeneous organic–inorganic hybrid polymer thin films were designed with improved mechanical properties and low dielectric constants (<3.0). Novel soluble siloxane–silsesquioxane hybrid polymers were synthesized with cyclic and/or cage silane monomers, which had triorganosiloxy ($R_3Si_{1/2}$), diorganosiloxane ($R_2SiO_{2/2}$), and organosilsesquioxane ($RSiO_{3/2}$) moieties with ethylene bridges at the molecular level, by the hydrolysis and condensation of 2,4,6,8-tetramethyl-2,4,6,8-tetra(trimethoxysilylethyl)cyclotetrasiloxane (a cyclic monomer). The electrical properties of these films, including the dielectric constant (~2.51), leakage current (6.4×10^{-11} A/cm^2 at 0.5 MV/cm), and breakdown voltage (~5.4 MV/cm) were fairly good. Moreover, the mechanical properties of the hybrid films, including the hardness (~7 GPa), modulus (~1.2 GPa), and crack-free thickness (<2 μm), were excellent in comparison with those of previous spin-on-glass materials with low dielectric constants. The excellent mechanical properties were proposed to be due to the high contents of Si—OH groups (>30%) and the existence of ethylene bridge and siloxane moieties in the hybrid polymer precursors. In addition, the mechanical properties of the hybrid films were affected by the contents of the cagelike structures. The more cagelike structures a hybrid film contained, the worse its mechanical properties were. © 2003 Wiley Periodicals, Inc. J Appl Polym Sci 90: 626–634, 2003

Key words: thin films; dielectric properties; spin coating; polycondensation; inorganic polymers

INTRODUCTION

As the feature size in integrated circuits continues to decrease, the reduced cross-sectional area of the interconnect increases the resistivity of metal lines, and the narrower spacing between the interconnects also increases the capacitance; this leads to severe performance limitations. Therefore, conventional interconnect materials such as aluminum-based and silicon dioxide-based dielectrics [dielectric constant (k) = 4.0–4.5] have been replaced by copper and low-k (low-dielectric) materials. Promising candidates for low-k applications include inorganic spin-on polymers, such as hydrogensilsesquioxane (k = 3.1), methylsilsesquioxane (MSQ; k = 2.7), and hybrid organic silsesquioxane polymer (k = 2.5), because they have excellent thermal stability up to 500°C as well as inherently low k values.[1] Moreover, thin films can easily be prepared by a simple spin-coating method with a silsesquioxane-based polymer, which can be prepared by an acid-catalyzed controlled hydrolytic polycondensation of alkyltrimethoxysilane.[2,3] However, the existence of Si—R (H and CH_3) bonds in these inorganic polymer films leads to a potential lack of mechanical stability for various semiconductor fabrication steps, such as chemical mechanical polishing (CMP).[4] Reliable inorganic thin films for chip integration are required to have high surface hardness as well as mechanical toughness to withstand such severe mechanical stress conditions.

Several studies have been performed for developing organic–inorganic hybrid materials with improved mechanical properties. Bridged polysilsesquioxanes are typical examples of homogeneous organic–inorganic hybrid materials made from precursors that integrate organic–inorganic groups on a molecular length scale.[5,6] Star gels, which have high levels of toughness, were developed by Sharp and Michalczyk.[7,8] These star gels were prepared from a monomer with a flexible built-in method on a molecular level.

Correspondence to: J.-H. Yim.

Journal of Applied Polymer Science, Vol. 90, 626–634 (2003)
© 2003 Wiley Periodicals, Inc.

Zhang et al.[9] showed various porous polyhedral silsesquioxane polymers synthesized by hydrosilylation with a platinum catalyst. However, it is difficult to make thin films with a sol–gel process in a large-scale-integration (LSI) process because of several problems, such as long reaction times for film formation, water absorption, film shrinkage, and metal corrosion.

In our study, we made several kinds of thin films from solutions of novel siloxane–silsesquioxane hybrid polymer precursors prepared with a simple spin-coating method to improve the mechanical properties while keeping k lower than 3.0. We compared the hardness (H) values, elastic modulus (E) values, and crack-free thicknesses of the films, measured with a nanoindentation method and image analysis, to investigate the effects of the molecular structures of the siloxane–silsesquioxane hybrid precursors. The electrical properties, such as the dielectric constant, leakage current, and breakdown voltage, of the hybrid films were also monitored.

EXPERIMENTAL

Materials

Silicon-based compounds such as methyltrimethoxysilane (monomer I; Strem Co., Tully Town, PA), trichlorosilane (Tokyo Chemical Industry Co., Tokyo, Japan), 2,4,6,8-tetramethyl-2,4,6,8-tetravinylcyclotetrasiloxane (Aldrich Chemical Co.), and octa(chlorosilylethyl)poly(oligosilsesquioxane) (Hybrid Plastic Co., Fountain Valley, CA) were used as received. Catalysts such as hydrochloric acid (Samchun Pure Chemical Co., Ltd., Seoul, Korea) and a platinum (*O*)-1,3-divinyl-1,1,3,3-tetramethyldisiloxane complex in xylene (Aldrich Chemical, Milwaukee, WI) were also used as received. Triethylamine (Aldrich Chemical), anhydrous sodium sulfate (Samchun Pure Chemical), methyl alcohol (Aldrich Chemical), and acetone (J.T. Baker, Phillipsburg, NJ) were used as received without further purification. Solvents such as tetrahydrofuran (J.T. Baker) and diethyl ether (J.T. Baker) were purified by distillation in the presence of sodium under an atmosphere of N_2.

Monomer synthesis

Synthesis of 2,4,6,8-tetramethyl-2,4,6,8-tetra (trimethoxysilylethyl)cyclotetrasiloxane (monomer II)

To a flask were added 29.014 mmol (10.0 g) of 2,4,6,8-tetramethyl-2,4,6,8-tetravinylcyclotetrasiloxane and 0.164 g of a platinum (*O*)-1,3-divinyl-1,1,3,3-tetramethyldisiloxane complex (a solution in xylene), and then the mixture was diluted with 300 mL of diethyl ether. Next, the flask was cooled to −78°C, 127.65 mmol (17.29 g) of trichlorosilane was slowly added, and the mixture was slowly warmed to room temperature. The reaction was continued at room temperature for 48 h, and any volatile materials were removed from the reaction mixture under a reduced pressure of about 0.1 Torr. To the mixture was added 100 mL of pentane; the mixture was stirred for 1 h and then was filtered through celite, providing a clear, colorless solution. The volatile materials were evaporated from the solution under a reduced pressure of about 0.1 Torr to afford 23.1 g of a colorless liquid compound, $[—Si(CH_3)(CH_2CH_2Cl_3)O—]_4$, in a yield of 90%.

The compound (11.28 mmol, 10.0 g) was diluted with 300 mL of tetrahydrofuran, and the flask was cooled to −78°C; 136.71 mmol (13.83 g) of triethylamine and 136.71 mmol (4.38 g) of methyl alcohol were added, and the mixture was slowly warmed again to room temperature. The reaction was continued at 50°C for 15 h; the mixture was filtered through celite for the removal of triethylamine hydrochloride salts, and then volatile materials were evaporated from the filtrate under a reduced pressure of about 0.1 Torr. Subsequently, 50 mL of pentane was added, and the mixture was stirred for 1 h. Then, the mixture was filtered through celite to provide a clear, colorless solution. The pentane was evaporated from this solution under a reduced pressure of about 0.1 Torr to afford 8.74 g of monomer II as a colorless liquid in a yield of 94%.

^{1}H-NMR (300 MHz, acetone-d_6, δ): 0.13 (s, 12H), 0.54–0.64 (m, 16H), 3.54 (s, 36H). ^{13}C-NMR (75 MHz, acetone-d_6, δ): −1.84 ($D_2^{(CH3)}$), 0.74 ($T_0^{(CH2)}$), 8.29 ($D_2^{(CH2)}$), 50.15 (—OCH_3). ^{29}Si-NMR (119.3 MHz, acetone-d_6, δ): −42.20 (T_0), −19.75 (D_2).

Synthesis of octa(methoxysilylethyl)octasilsesquioxane (monomer III)

To a flask was added 7.19 mmol (10.0 g) of octa(chlorosilylethyl)poly(oligosilsesquioxane), and this was diluted with 300 mL of tetrahydrofuran. Next, the flask was cooled to −78°C, 64.73 mmol (6.55 g) of triethylamine and 64.61 mmol (2.07 g) of methyl alcohol were added, and the mixture was slowly warmed again to room temperature. The reaction was continued at room temperature for 20 h; the mixture was filtered through celite for the removal of triethylamine hydrochloride salts, and then volatile materials were evaporated from the filtrate under a reduced pressure of about 0.1 Torr. To the mixture was added 100 mL of pentane; the mixture was stirred for 1 h and then was filtered through celite to provide a clear, colorless solution. The pentane was evaporated from the solution under a reduced pressure of about 0.1 Torr to afford 8.5 g of monomer III as a white powder in a yield of 87.3%.

^{1}H-NMR (300 MHz, acetone-d_6, δ): 0.15 (s, 48H), 0.60–0.73 (m, 32H), 3.44 (s, 24H). ^{13}C-NMR (75 MHz,

TABLE I
Summary of the Monomer Compositions of the Reactant and the Yield

	Monomer I		Monomer II		Monomer III		
Precursor	mmol	g	mmol	g	mmol	g	Yield (g)
A	36.71	5.00	—	—	—	—	2.3
B	—	—	10.80	9.00	—	—	5.7
C	36.71	5.00	4.08	3.40	—	—	3.8
D1	—	—	10.80	9.00	1.20	1.63	6.5
D2	—	—	10.80	9.00	4.63	6.28	8.1

Reaction conditions: r_1 [HCl]/[Si—OMe] = 0.01; r_2 [H_2O]/[Si—OMe] = 3.33; reaction temperature = 70°C, polymerization time = 16 h. r_1 = mole ratio of HCI and Si—OH group in Monomer, r_2 = mole ratio of H_2O and Si—OH group in monomer.

acetone-d_6, δ): −3.49 ($M_0^{(CH3)}$), 3.86 ($T_0^{(CH2)}$), 7.39 ($M_0^{(CH2)}$), 49.96 (—OCH_3). ^{29}Si-NMR (119.3 MHz, acetone-d_6, δ): −65.91 (T_3), 18.62 (M_0).

Preparation of the precursors

Synthesis of precursor A

To a flask was added 36.71 mmol (5.00 g) of monomer I, and this was diluted with 100 mL of tetrahydrofuran. Next, a diluted HCl solution (1.10 m*M* hydrochloride) prepared by the dilution of concentrated HCl (35 wt % hydrochloride) with deionized water was slowly added at −78°C, followed by the addition of more deionized water, so that the total amount of water, including the inherent water in the added diluted HCl solution, was 367.02 mmol (6.606 g). Thereafter, the flask was slowly warmed to 70°C, and the mixture was allowed to react for 16 h. Then, the reaction mixture was transferred into a separatory funnel, 180 mL of diethyl ether was added, and then the mixture was rinsed three times with 50 mL of deionized water. Subsequently, 5 g of anhydrous sodium sulfate was added, and the mixture was stirred at room temperature for 5 h to remove any traces of water; it was then filtered to provide a clear, colorless solution. Any volatile materials were evaporated from this solution under a reduced pressure of about 0.1 Torr to afford 2.7 g of crude precursor A as a white powder. After the produced white power was dissolved in 5 mL of acetone, residual particles were eliminated with a mem-

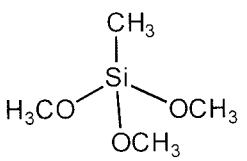

Monomer I

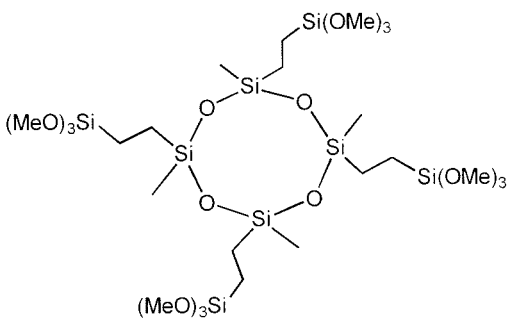

Monomer II

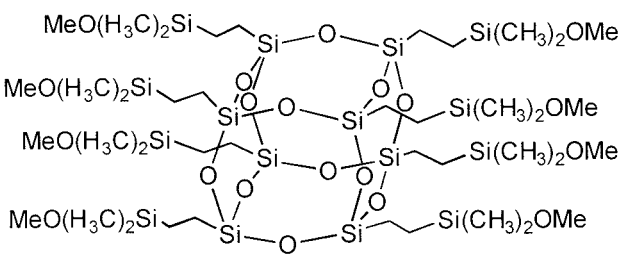

Monomer III

Figure 1 Structures of the cyclic and cage monomers: (a) monomer I, (b) monomer II, and (c) monomer III.

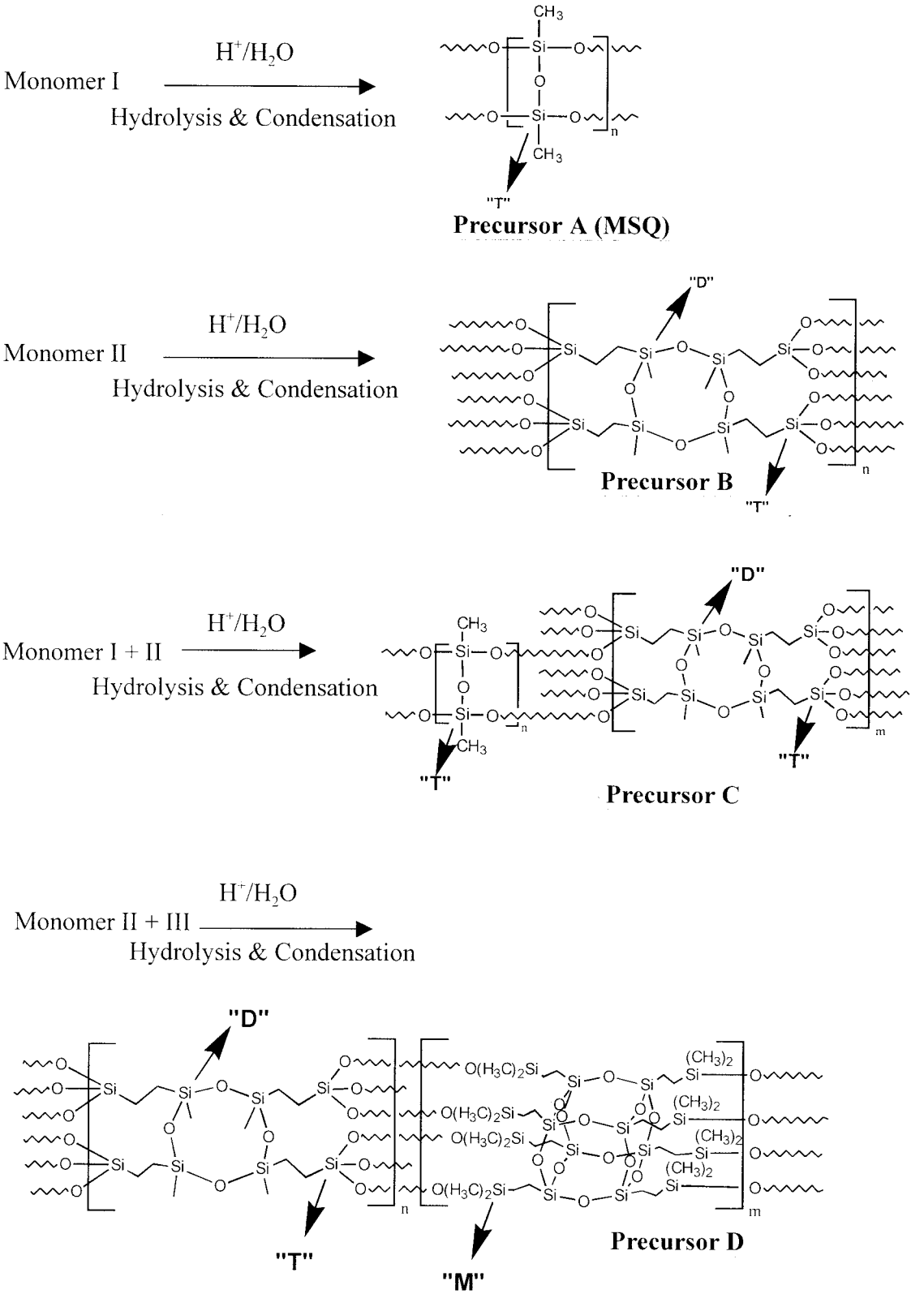

Scheme 1 Systematic design of the siloxane–silsesquioxane hybrid precursors.

TABLE II
Content of the Functional Groups and Molecular Weights of Various Precursors

Precursor	Monomer (molar fraction) I	II	III	Si—OH[a] (mol %)	Si—OMe[a] (mol %)	Si—CH_3[a] (mol %)
A	1.0	—	—	12.4	1.2	86.4
B	—	1.0	—	35.3	0.9	63.8
C	0.9	0.1	—	39.8	0.5	59.7
D1	—	0.9	0.1	26.6	—	73.4
D2	—	0.7	0.3	18.9	0.7	80.4

Reaction conditions: r_1 [HCl]/[OMe] = 0.01; r_2 [H_2O]/[OMe] = 3.333;70°C; 16 h.

[a] Measured by ^{1}H-NMR: Si—OH (%) = Area(Si—OH)/[Area(Si—OH) + Area(Si—OCH_3)/3 + Area(Si—CH_3)/3] × 100; Si—OCH_3 (%) = Area(Si—OCH_3)/3/[Area(Si—OH) + Area(Si—OCH_3)/3 + Area(Si—CH_3)/3] × 100; Si—CH_3 (%) = Area(Si—CH_3)/3/[Area(Si—OH) + Area(Si—OCH_3)/3 + Area(Si—CH_3)/3] × 100.

brane filter (0.2 μm). The acetone was evaporated from the solution under a reduced pressure of about 0.1 Torr to afford 2.3 g of precursor A as a white powder.

Synthesis of precursors B–D

Precursor B, precursor C, and precursor D were prepared with a synthetic method similar to that of precursor A. The polymerization conditions are summarized in Table I.

Characterization of the precursors

The monomer and precursor samples were dissolved in deuterated acetone (acetone-d6). The microstructures of the monomer and precursors were analyzed with ^{1}H-NMR, ^{13}C-NMR (Bruker AM300, Billerica, MA) and ^{29}Si-NMR (Bruker DMX600). The chemical shifts are reported as δ units (ppm) relative to tetramethylsilane. The powder samples of the cured precursors for the solid-state ^{29}Si-NMR experiments were prepared at 420°C under N_2. The solid-state ^{29}Si-NMR experiments were performed at 79.5 MHz with a Bruker DSX 400 spectrometer with a 4-mm magic-angle-spinning probe and a spinning-speed regulation of 12 kHz.

Preparation of the thin films

The precursor solutions were prepared by mixing of the siloxane–silsesquioxane hybrid polymer and propylene glycol monomethylether acetate in agreement with an adequate ratio. These compositions were applied to spin coating at 3000 rpm for 13 s onto p-type silicon wafers doped with boron. The coated substrates were then subjected to soft baking on a hot plate for 1 min at 150°C and for another minute at 250°C, so that the organic solvent would sufficiently be removed. The substrates so prepared were cured in a cylindrical furnace (Linberg 55642, Water Town, WI) at 420°C for 60 min under vacuum conditions.

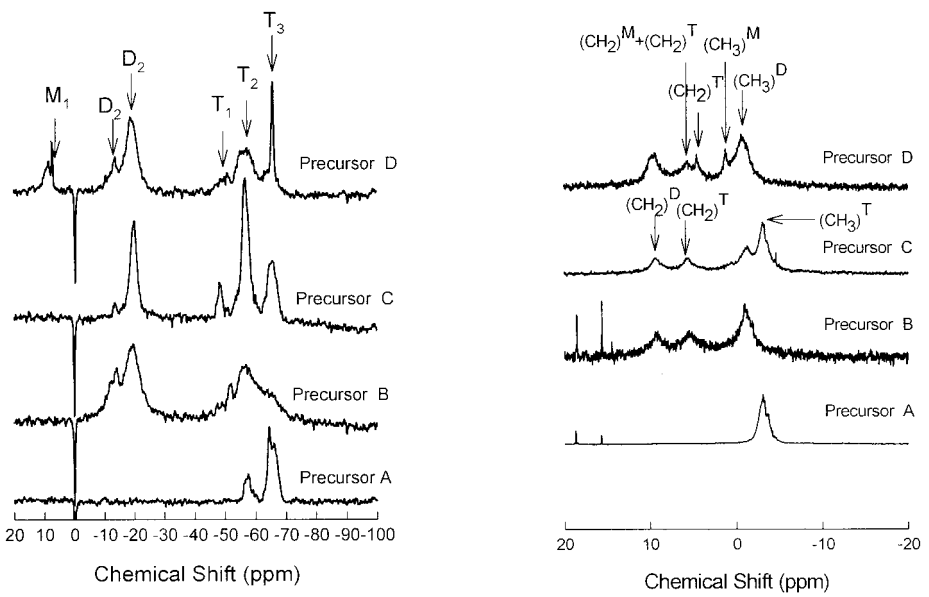

Figure 2 (a) ^{29}Si-NMR and (b) ^{13}C-NMR spectra of precursors A–D.

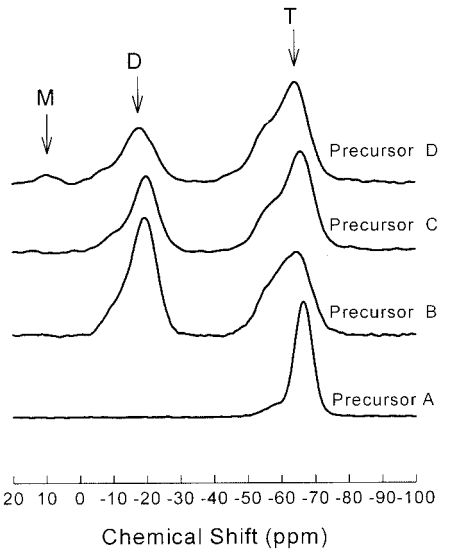

Figure 3 ^{29}Si CP-MAS NMR spectra of precursors A–D.

Characterizations of the low-*k* thin films

The refractive indices and thicknesses of the thin films were measured with a 2010 prism coupler (Metricon Co., Pennington, NJ) and a P-10 surface profiler (Tencor, San Jose, CA). The film densities were measured by Rutherford backscattering Spectrometry (RBS) with 3.6-MeV $^4He^+$ ions. The *H* and *E* values of the hybrid polymer films were measured with the continuous stiffness measurement by nanoindentation method.[10] In this technique, the force required as a function of the indentation depth is recorded while a three-sided Berkovich diamond indenter is pushed into the sample and then withdrawn, and the contact stiffnesses for all depths are measured by the superimposing of a small oscillation to the force signal at a relatively high frequency. The amplitude and frequency employed for this experiment were 1 nm and 45 Hz, respectively. Multiple points (typically six points) on each sample were indented, and the results for *H* and *E* were averaged for ensured reliability.

H was calculated by its normal definition:

$$H = \frac{F_{\max}}{A} \tag{1}$$

where $F_{\max}$ is the peak indentation load and *A* is the projected area of the hardness impression. For the *E* calculation, Sneddon's solution[11] was adapted:

$$E_r = \frac{1}{\beta}\frac{\sqrt{\pi}}{2}\frac{S}{\sqrt{A}} \tag{2}$$

where *S* is the stiffness and *A* is the contact area. β is a shape correction factor for the indenter shape (β = 1.034 for a Berkovich tip, which is used in this study). To account for the elastic response of the indenter, we assumed that the modulus in eq. (2) was a reduced modulus (E_r) defined as follows:

$$\frac{1}{E_r} = \frac{1-\nu_{\text{indenter}}^2}{E_{\text{indenter}}} + \frac{1-\nu_{\text{film}}^2}{E} \tag{3}$$

where *E* and ν_{film} are Young's modulus and Poisson's ratio for the film, respectively, and E_{indenter} and ν_{indenter} are Young's modulus and Poisson's ratio of the indenter, respectively.

k was measured at a frequency of 100 kHz with an HP 4284 (Palo Alto, CA) with a metal–insulator–metal (MIM) structure. The leakage current density and breakdown voltage were measured with a Keithley 237 (Cleveland, OH) source measure and an HP 4155B (Palo Alto, CA), respectively, with a metal–insulator–semiconductor (MIS) structure. In both MIM and MIS structures, for a top electrode with a diameter of 1 mm, aluminum metal was deposited by an electron-beam evaporation method. The leakage current density value was taken at an electric field of 0.5 MV/cm, and the breakdown voltage value was obtained at a compliance current of 10 mA.

RESULTS AND DISCUSSIONS

Design of the siloxane–silsesquioxane hybrid precursors

Three kinds of monomers were used to make the organic soluble precursors shown in Figure 1. The microstructures of the silicone-based polymers are classified by the number of Si—O moieties: M for a triorganosiloxy ($R_3Si_{1/2}$) unit, D for a diorganosiloxane ($R_2SiO_{2/2}$) unit, T for an organosilsesquioxane ($RSiO_{3/2}$) unit, and Q for a silicate($SiO_{4/2}$) unit.[12,13] Monomer I, which can produce a T structure, has three reactive methoxy groups; monomer II has a cyclic structure containing D and T moieties and 12 methoxy groups; and monomer III has a cage structure containing M and T moieties and eight reactive methoxy groups. We prepared MSQ (precursor A) and three kinds of siloxane–silsesquioxane hybrid precursors with the monomers through hydrolysis/condensation reactions in the presence of an acid catalyst, as shown in Scheme 1.

Table II shows the contents of Si—OH groups and Si—OMe groups and the molecular weights of the various precursors. The contents of the Si—OH groups are greater than 35 mol % for the precursors prepared by MTMS (monomer I) and cyclic monomer (monomer II). This might be due to the less condensed structure of the precursors prepared with monomer II, which has 12 methoxy groups. In general, Si—OH groups can effectively form dense thin films after the curing process.

TABLE III
Basic Properties of Various Thin Films Prepared with Hybrid Precursors

Precursor	Monomer (molar fraction) I	II	III	Refractive index[a]	C/Si ratio[b]	Density (g/cm^3)[b]	Contact angle (θ)
A	1.0	—	—	1.378 ± 0.004	3.00	1.06	88.9 ± 0.91
B	—	1.0	—	1.440 ± 0.001	3.50	1.43	96.5 ± 1.03
C	0.9	0.1	—	1.414 ± 0.001	3.05	1.19	97.5 ± 1.15
D1	—	0.9	0.1	1.429 ± 0.001	3.65	1.24	96.3 ± 0.86
D2	—	0.7	0.3	1.431 ± 0.001	3.95	1.21	99.4 ± 1.97

[a] The refractive index and thickness were measured with a prism coupler.
[b] Film density was measured by RBS with 3.6-MeV $^4He^+$ ions.

Figure 2 shows the ^{29}Si-NMR and ^{13}C-NMR spectra of the prepared precursors in acetone-d_6. For precursor A (MSQ), relatively sharp signals due to T^2 and T^3 can be observed at −56 and −65 ppm, respectively, and major signals are due to a T^3 peak. The broad signals due to $(CH_3)^T$ can be observed at −3 ppm only. The degree of crosslinking (DC) of precursor A may be the highest for the prepared precursors. For precursors B and C, the broad signals due to D^2, T^1, T^2, and T^3 can be observed at −13 to −19, −48, −56, and −65 ppm, and major signals are due to a T^2 peak.

This means that the structures of precursors B and C have a lower DC at the precursor state than those of precursor A. The signals due to $(CH_3)^T$, $(CH_3)^D$, $(CH_2)^T$, and $(CH_2)^D$ can be observed at −3.0, −1.0, 5.5, and 9.1 ppm, respectively, in the ^{13}C-NMR spectrum. The D^2, $(CH_2)^T$, and $(CH_2)^D$ peaks might be from cyclic and ethylene bridges of monomer II. For precursor D, one more signal due to M can be observed around 8–9 ppm, and major signals are due to a T^2 peak. From the results of NMR analysis, it is postulated that the structures of precursors B, C, and D are less condensed than that of precursor A (MSQ). These results correlate well with the contents of Si—OH groups, as shown in Table II.

To determine the structures of the cured films, we thermally treated powders of precursors A–D at 420°C for 1 h *in vacuo*. Figure 3 shows ^{29}Si cross-polarity/magic-angle-spinning (CP-MAS) NMR spectra of condensed powders of precursors A–D. The major peak of all the precursors is T^3 as anticipated. This means that T^1 and T^2 structures, which have Si—OH end groups, transform into T^3 during vacuum curing. However, precursors B and C still have a D structure that comes from the siloxane linkage of monomer II after vacuum curing. Additionally, precursor D has an M structure that comes from monomer III after vacuum curing. Therefore, it seems that the unique D and M structures of precursors B, C, and D are sustained in the cured thin films.

Properties of the siloxane–silsesquioxane hybrid films

The refractive indices of the films made from cyclic and/or cage-containing precursors are much higher

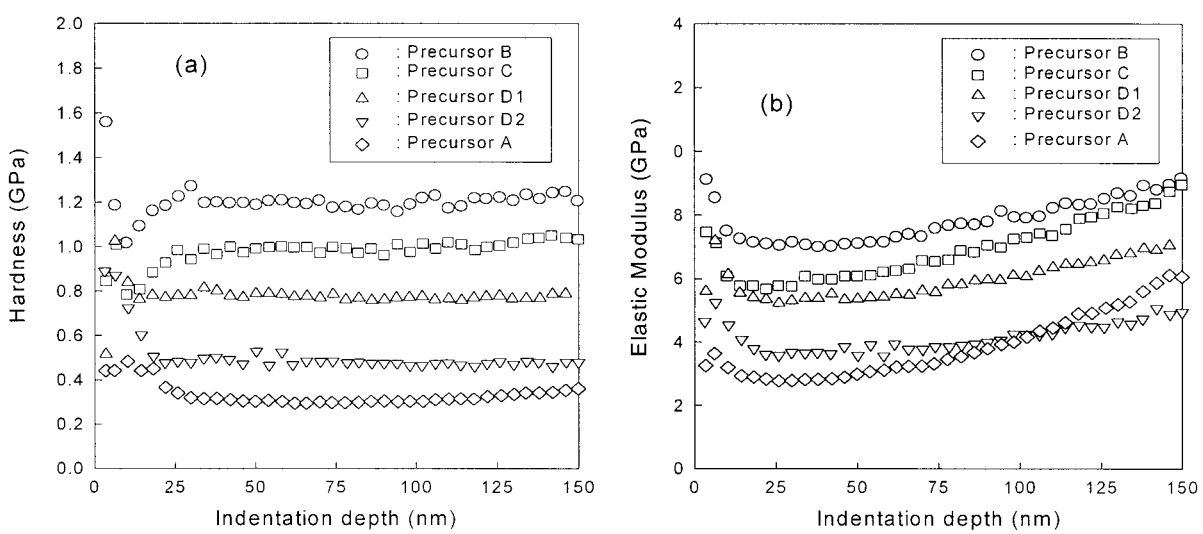

Figure 4 (a) *H* and (b) *E* values, plotted as functions of the indentation depth, of low-*k* films prepared with various hybrid precursors on silicon substrates.

TABLE IV
***H* and *E* values of Low-*K* Thin Films Prepared with Various Hybrid Precursors**

Precursor	*H* (GPa)[a]	*E* (GPa)[a]	Crack-free thickness (μm)	Thickness (Å)[b]
A	0.30 ± 0.03	2.98 ± 0.29	< 0.8	6602 ± 86
B	1.26 ± 0.11	7.38 ± 0.33	< 2.0	9847 ± 14
C	0.99 ± 0.07	6.09 ± 0.23	< 1.5	8143 ± 22
D1	0.79 ± 0.06	5.37 ± 0.24	< 1.2	10124 ± 17
D2	0.53 ± 0.09	3.58 ± 0.28	< 1.2	10519 ± 38

[a] *H* and *E* values of all films were collected at an indentation depth of 50 nm.
[b] Thickness data were measured by means of a prism coupler.

than the indices of those made from precursor A, as shown in Table III. This might be due to the relatively higher contents of carbon and densities of the films made from organic–inorganic hybrid precursors. The contact angles of the films obtained from organic–inorganic hybrid precursors are much higher than the angles of that made from precursor A (MSQ). The films prepared from organic–inorganic hybrid precursors have hydrophobic surfaces because of the high contents of carbon (C/Si ratio) in comparison with precursor A. Therefore, the hybrid films with 2,4,6,8-tetramethyl-2,4,6,8-tetra(trimethoxysilylethyl)cyclotetrasiloxane may have strong resistance to wet chemicals such as photoresist stripping solutions, CMP aqueous slurries, and cleaning water that are used in semiconductor processes.

Figure 4 compares the *H* and *E* values of the films on a silicon substrate made from different precursors. The results are an average of six indentations made to a depth of 150 nm and have been plotted as a function of the indentation depth. Both *H* [Fig. 4(a)] and *E* [Fig. 4(b)] fluctuate or decrease with an increasing depth of indentation at small depths (<25 nm). This observation might be explained by the complex effect of the indentation size[14] and intrinsic surface properties. *H* is constant for all the films at depths between 25 and 125 nm and then increases little by little with an increasing depth of indentation. The *E* values of all the films also show plateaus, but for a relatively narrow depth range between 25 and 45 nm, and then they start to increase. The observed increases in *H* and *E* are due to the influence of the silicon substrate ($E \sim 174$ GPa and $H \sim 12.5$ GPa). Compared with *H*, the measured *E* values are more strongly affected by the substrate. This is to be expected because the elastic field under the indenter is not confined to the film itself; it is a longer range field than the plastic field that extends into the substrate. The observation of the indentation size and intrinsic property effects at shallow depths and substrate effects at large depths complicates the identification of the true *H* and *E* values of the films. The plateaus that we have identified in curves of *H* and *E* versus the depth may be influenced by the competition between these effects. However, considering the relatively shallow indentation depth of less than 150 nm compared with the film thickness of approximately 1 μm (except for precursor A) and the soft and compliant properties of the films compared with those of the silicon substrate, we think these plateaus might be good estimates of the true properties of the films. Even the plateau of *E* of the film made from precursor A might be used for comparison because it shows the lowest value. The *H* and *E* values of these films at an indentation depth of 40 nm are summarized in Table IV.

Figure 4 and Table IV show that a precursor with a higher molar percentage of Si—OH terminal bond tends to yield higher *H* and *E* values. This result indicates that a higher density of a hybrid film due to a larger amount of Si—OH terminal bond in the precursors improves the mechanical properties of the hybrid film dominantly. Lu et al.[15] reported a consistent trend of increasing *H* and *E* values with the substitution of bridged silsesquioxane for siloxane. Therefore, the other reason for the enhancement of the mechanical properties is the existence of flexible ethylene bridges and D structures from comparisons between precursors B and C. For precursor D, however, the *H* and *E* values decrease as the content of the cage monomer (monomer III) increases. This result suggests that a cagelike structure could be act as a defect in the siloxane crosslinked network. Therefore, a cagelike structure is not desirable in terms of the mechanical properties in hybrid thin films.

Table V presents a summary of the electrical properties of thin films made from precursors B and C. The *k* value of a thin film for precursor B is 2.51, whereas *k* is 2.67 for precursor C. This implies that the involvement of the D structure originating from monomer II contributes significantly to lowering the *k* value of the thin film. It is postulated that the D structure originating from monomer II may induce a more porous structure because of the formation of interpore and intrapore voids.[7] The dissipation factor remains low (0.002) for these precursors, and this is acceptable even for applications to interlayers of LSI devices.[16] The measured leakage current densities of the thin films for B and C are 6.9×10^{-11} and 6.4×10^{-11} A/cm^2 at

TABLE V
Electrical Properties of Various Thin Films Prepared with Hybrid Precursors

Precursor	k[a]	Dissipation factor	Leakage current (A/cm^2 at 0.5 MV/cm)	Breakdown voltage (MV/cm)
B	2.51	0.002	6.9×10^{-11}	5.4
C	2.67	0.002	6.4×10^{-11}	5.7

[a] Measured by MIM.

0.5 MV/cm, respectively. These leakage current density values are also acceptable for applications to LSI devices because the leakage current density of SiOF films ($k \sim 3.5$) has been reported to remain around 10^{-10} A/cm^2, and this has been used widely in real LSI devices in recent years.[17] The breakdown voltages for precursors B and C are 5.4 and 5.7 MV/cm, respectively, which are comparable to those of SiOF films.[16]

CONCLUSIONS

Hybrid films, which had D and T moieties with ethylene bridges at a molecular level, were prepared by a simple spin-coating method with soluble siloxane–silsesquioxane hybrid polymers synthesized from the hydrolysis and condensation of 2,4,6,8-tetramethyl-2,4,6,8-tetra(trimethoxysilylethyl)cyclotetrasiloxane (a cyclic monomer). The electrical properties of the films, including the dielectric constant, leakage current, and breakdown voltage, were acceptable for applications to LSI devices. The excellent mechanical properties of the hybrid films were due to high contents of Si—OH groups (>30%) and the existence of ethylene bridges and siloxane (D) moieties in the hybrid polymer precursors. The cagelike structure of low-k films was not desirable in terms of mechanical properties such as the hardness, modulus, and toughness.

References

1. Hacker, N. P. MRS Bull 1997, 22(10), 33.
2. Takamura, N.; Gunji, T.; Hatano, H.; Abe, Y. J Polym Sci Part A: Polym Chem 1999, 37, 1017.
3. Abe, Y.; Hatano, H.; Gunji, T. J Polym Sci Part A: Polym Chem 1995, 33, 751.
4. Cook, R. F. Mater Res Soc Symp Proc 1999, 576, 301.
5. Shea, K. J.; Loy, D. A. MRS Bull 2001, 26(5), 368.
6. Shea, K. J.; Loy, D. A.; Webster, O. J Am Chem Soc 1992, 114, 6700.
7. Sharp, K. G.; Micalczyk, M. J. Mater Res Soc Symp Proc 1996, 435, 105.
8. Sharp, K. G.; Micalczyk, M. J. J Sol-Gel Sci Technol 1997, 8, 541.
9. Zhang, C.; Babonneau, F.; Bonhomme, C.; Laine, R. M.; Soles, C. L.; Hristov, H. A.; Yee, A. F. J Am Chem Soc 1998, 120, 8380.
10. Oliver, W. C.; Pharr, G. M. J Mater Res 1992, 7, 1564.
11. Sneddon, I. N. Int J Eng Sci 1965, 3, 47.
12. Arkles, B. MRS Bull 2001, 26(5), 402.
13. Baney, R. H.; Itoh, M.; Sakakibara, A.; Suzuki, T. Chem Rev 1995, 95, 1409.
14. Nix, W. D.; Gao, H. J Mech Phys Solids 1998, 46, 411.
15. Lu, Y.; Fan, H.; Doke, N.; Loy, D. A.; Assink, R. A.; La Van, D. A.; Brinker, C. J. J Am Chem Soc 2000, 122, 5258.
16. Singer, P. Semicond Int 1996, May 1, 88.
17. Lee, S.; Yoo, J.; Oh, K.; Park, J. Mater Res Symp Proc 1997, 476, 291.